

New Moscovian palaeomagnetic pole from the Edjeleh fold (Saharan craton, Algeria)

M. E. M. Derder, B. Henry, B. Bayou, H. Djellit, M. Amenna

▶ **To cite this version:**

M. E. M. Derder, B. Henry, B. Bayou, H. Djellit, M. Amenna. New Moscovian palaeomagnetic pole from the Edjeleh fold (Saharan craton, Algeria). Geophysical Journal International, 2001, 147, pp.343-355. 10.1046/j.0956-540X.2001.01530.x . insu-03597748

HAL Id: insu-03597748

https://insu.hal.science/insu-03597748

Submitted on 4 Mar 2022

HAL is a multi-disciplinary open access archive for the deposit and dissemination of scientific research documents, whether they are published or not. The documents may come from teaching and research institutions in France or abroad, or from public or private research centers.

L'archive ouverte pluridisciplinaire **HAL**, est destinée au dépôt et à la diffusion de documents scientifiques de niveau recherche, publiés ou non, émanant des établissements d'enseignement et de recherche français ou étrangers, des laboratoires publics ou privés.



Distributed under a Creative Commons Attribution| 4.0 International License

Geophys. J. Int. (2001) **147,** 343–355

New Moscovian palaeomagnetic pole from the Edjeleh fold (Saharan craton, Algeria)

M. E. M. Derder,[1] B. Henry[2], B. Bayou,[1] H. Djellit[1] and M. Amenna[1]

[1] *Centre de Recherche en Astronomie Astrophysique et Géophysique (C.R.A.A.G.),* B.P. 63, 16340 *Bouzaréah, Alger, Algeria. E-mail: mderder@hotmail.com*

[2] *Géomagnétisme et Paléomagnétisme, IPGP and CNRS,* 4 *avenue de Neptune,* 94107 *Saint Maur cedex, France. E-mail: henry@ipgp.jussieu.fr*

Accepted 2001 June 6. Received 2001 May 16; in original form 1999 July 14

SUMMARY

A palaeomagnetic study was carried out in the Moscovian ($\sim$305 Ma) formation in the Edjeleh anticline, the only area where important dips can be observed in the Upper Palaeozoic series of the Illizi basin (Algeria). This study shows the existence of three magnetization components. Two of them are interpreted as Cenozoic and Permian remagnetizations; their poles are 88.8°N, 164.0°E, $K=262$, $A_{95}=3.3°$ and 43.4°S, 61.7°E, $K=93$, $A_{95}=5.9°$, respectively. The third component is determined by both well-defined ChRMs and remagnetization circles analysis. Its associated fold test is positive and significant. Because the folding started before or during the Autunian, this third component was acquired very early and is very probably the primary magnetization. Its corresponding palaeomagnetic pole (28.3°S, 58.9°E, $K=157$, $A_{95}=4.2°$) is close to the poles from the Saharan platform obtained from neighbouring periods. The positive fold test of this study thus validates these previous Upper Palaeozoic poles.

This new result is in agreement with the geodynamical model (Matte 1986; Henry *et al.* 1992), which proposed the occurrence of a large clockwise rotation of Africa during the Carboniferous; such a motion agrees with the Permian Pangaea A2 reconstruction.

Key words: Africa, apparent polar wander path, fold test, Moscovian, palaeomagnetic pole, Saharan craton.

INTRODUCTION

In order to improve the African palaeomagnetic database for Palaeozoic times, which is still poor, we have undertaken, during the last 10 years, systematic palaeomagnetic studies of the dated tabular formations of the Illizi basin (SE Algeria, Fig. 1a). Levels of various ages, ranging from the Silurian to the Albian, were analysed. These studies led to the determination of five new African palaeomagnetic poles. The first, determined in the 'El Adeb Larache' area, is of Moscovian age (Henry *et al.* 1992), the second is of Stephano–Autunian age from the Tiguentourine Formation (Derder *et al.* 1994a), the third is from the Middle Zarzaïtine Formation of Liassic–Dogger age (Derder *et al.* 1994b), the fourth, determined in the 'la Reculée' area from the Lower Zarzaitine is of Triassic–Liassic age (Kies *et al.* 1995), and the fifth is of Bashkirian age from the Oubarakat Formation (Derder *et al.* 2001a). These studies also showed the existence of Cenozoic and Permian remagnetization events.

However, as in most of the palaeomagnetic studies in horizontal tabular areas, the age of the magnetization acquisition has not been demonstrated. Indeed, in all cases, geological and geophysical constraints did not permit palaeomagnetic tests, except a reversal test in the Lower Zarzaïtine Formation of Triassic–Liassic age (Kies *et al.* 1995). Such a reversal test is not absolute proof of the primary character of the magnetization, but indicates that the magnetization consists of a single component. The only argument in favour of the primary character of the magnetization is the variation of its direction from one formation to another, while the magnetic overprints (Permian and Cenozoic) observed at some levels have the same orientation in the different geological formations.

To validate the previous results by a fold test, a new study was carried out 60 km SE of In Amenas city, in the Edjeleh region (27.4°N, 9.5°E, Fig. 1a), where important dips can be observed in Upper Palaeozoic formations of the Illizi basin (Fig. 1b). The Edjeleh anticline affects the Moscovian and the Stephano–Autunian formations, but only the Moscovian facies (El Adeb Larache Formation) appeared to be suitable for palaeomagnetic study.

GEOLOGICAL SETTING

The Edjeleh area is an anticline with a N–S axis that shows in its central part the northern outcrops of the Saharan Palaeozoic

© 2001 RAS

Downloaded from https://academic.oup.com/gji/article/147/2/343/718535 by guest on 04 March 2022

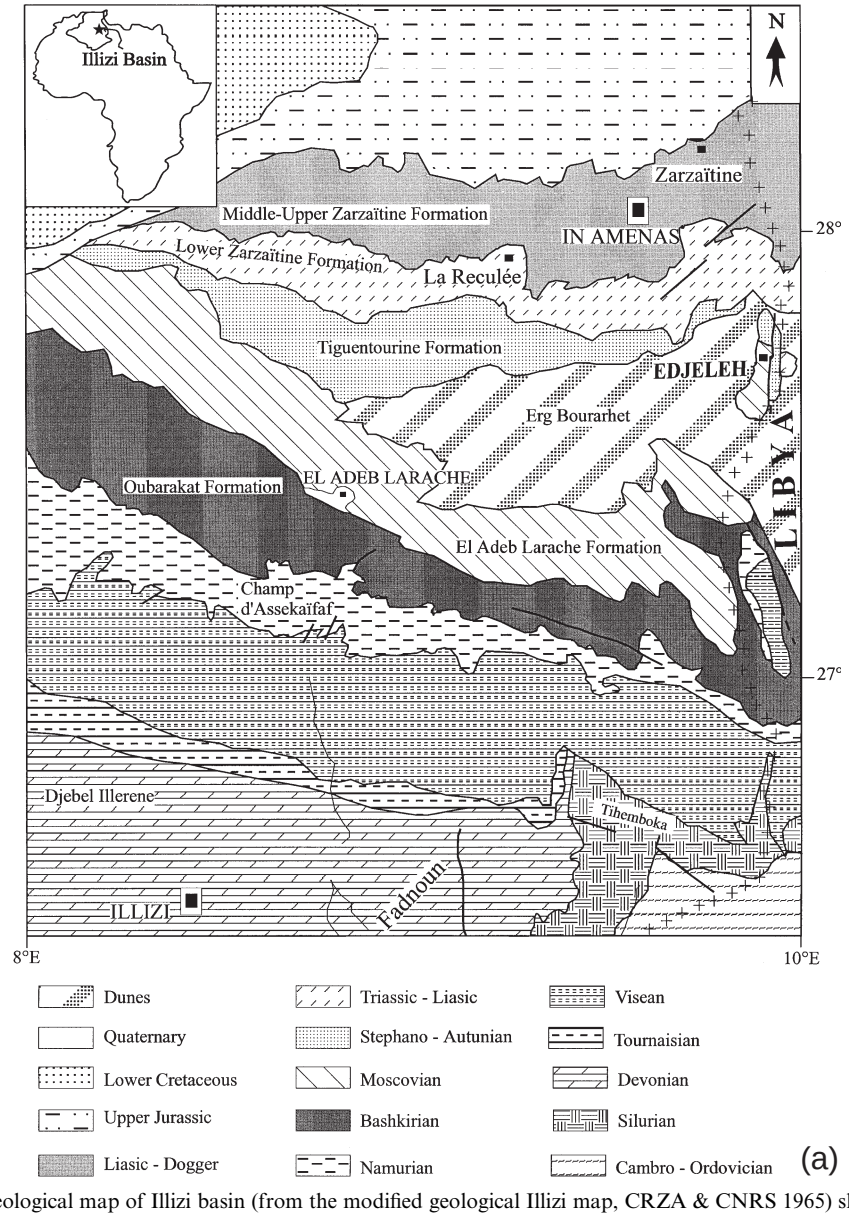


Figure 1. (a) Simplified geological map of Illizi basin (from the modified geological Illizi map, CRZA & CNRS 1965) showing the locations of the different geological formations studied in previous palaeomagnetic studies. (b) Locations of the studied Moscovian formation (from the modified geological Illizi map, CRZA & CNRS 1965) and of the sampling sites (stars). Locations of the different sedimentary basins in the Algerian Sahara. (c) Geological cross-section A–B (see b) of the Edjeleh area. (d) Stratigraphic column of the geological formation studied showing the locations of the sampling sites.

series of the Illizi basin. These series include the Moscovian marine formation of El Adeb Larache and the Stephano–Autunian Tiguentourine Formation, and are covered by the Triassic Zarzaïtine Formation (Figs 1b and c). This anticline has an asymmetrical shape. The western limb shows beds with very low dip values (0°–6°). The outcropping series of the eastern limb are more reduced and are affected by a reverse fault; the observed dip values are high (20°–80°).

The Moscovian series contain (de Lapparent 1949) many fossils: *Spirifer*, *Goniatites* and *Bellerophon* (Durif 1959; Legrand-Blain 1980) of Moscovian age (~305 Ma; Odin 1994). Two principal parts can be distinguished (Figs 1b and d): the bottom is characterized by centimetric levels of blue–violet limestones and the upper part consists from the base to the top of blue limestones, blue marly limestones with slumps and rich fossiliferous levels ('*Lumachelle* with *Goniatites*'), bioturbated green calcareous beds (thickness 0.3–0.5 m) with thinly bedded sandstones, and finally green calcareous rocks (Fig. 1d). All the upper series also contain many levels of rubefied red clay horizons.

The Moscovian is covered conformably by the Stephano–Autunian Tiguentourine Formation. The abnormal overlapping of several levels of the Moscovian by the Tiguentourine at Edjeleh is due to a later local backthrusting movement connected to the major fault (Fig. 1c).

The Moscovian levels and the Stephano–Autunian Tiguentourine Formation (Attar *et al.* 1981) were affected by folding (Figs 1b and c). The Lower Zarzaitine Formation of Upper Triassic age (Achab 1970) lays unconformably over the folded Tiguentourine Formation (Fig. 1d); therefore the main part of the deformation at least occurred before the Upper Triassic.

Downloaded from https://academic.oup.com/gji/article/147/2/343/718535 by guest on 04 March 2022

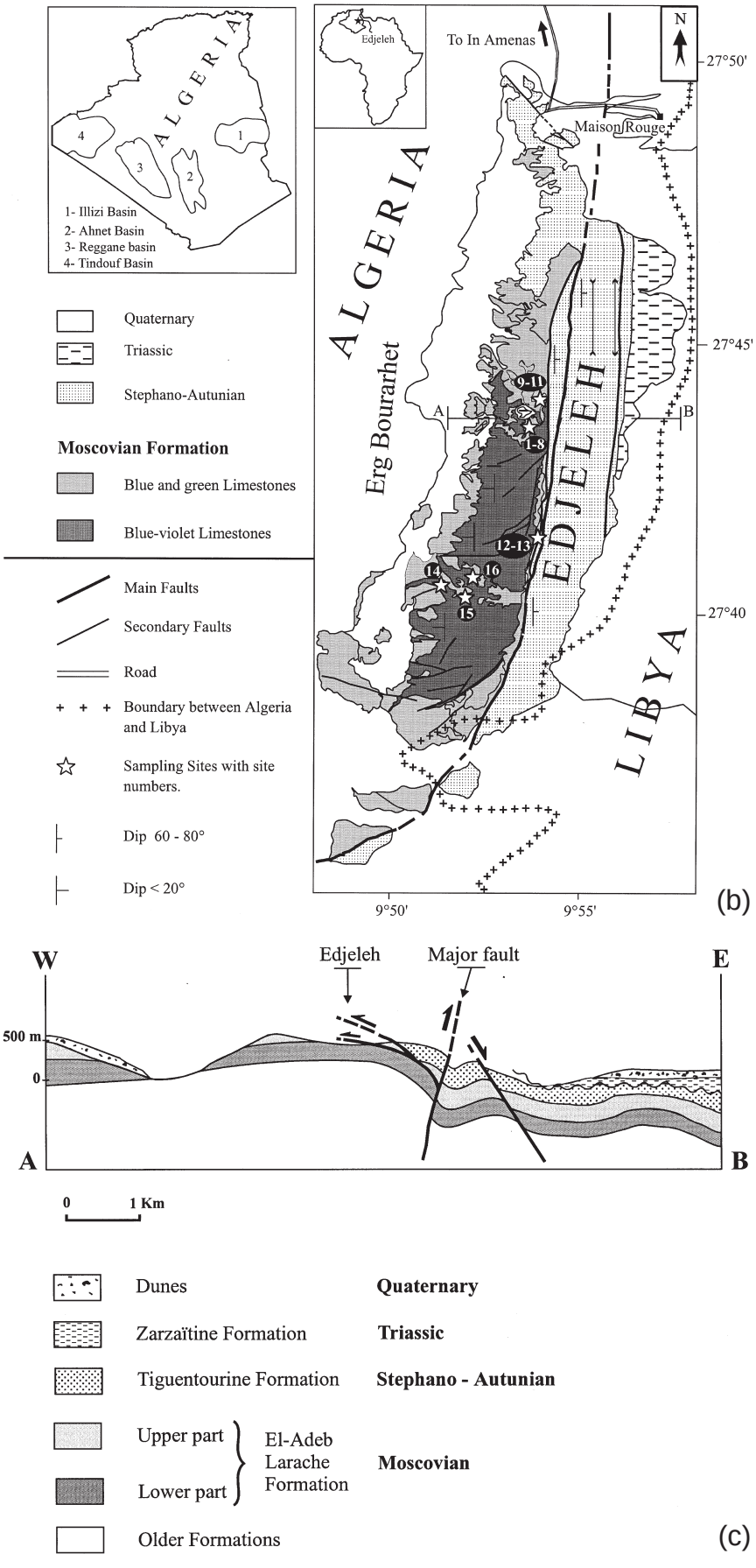


Figure 1. (*Continued.*)

Downloaded from https://academic.oup.com/gji/article/147/2/343/718535 by guest on 04 March 2022

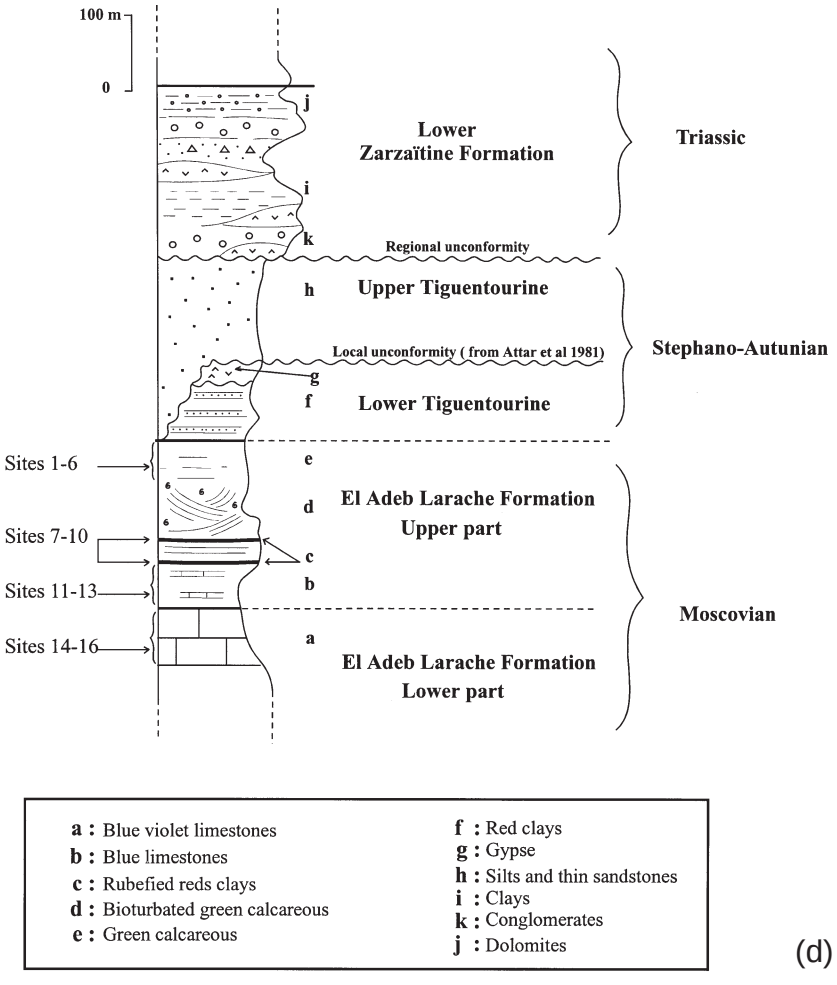


Figure 1. (*Continued.*)

However, as the Upper Tiguentourine levels are also locally discordant (Fig. 1d) on the Lower Tiguentourine levels (Attar *et al.* 1981), and as the Lower Tiguentourine is very reduced in thickness or even missing at the Edjeleh anticline, the folding started before or during the Stephano–Autunian.

SAMPLING AND ANALYSIS PROCEDURE

The sampling sites were located in the Edjeleh region, in the eastern part of the Illizi basin (Fig. 1a), approximately 70 km east of the El Adeb Larache locality where the previous Moscovian study was undertaken (Henry *et al.* 1992).

All the Moscovian outcropping levels at Edjeleh have been sampled (Fig. 1b): sites 1–6 in the green calcareous rocks, 7–10 in the rubefied red clay levels, sites 11–13 in the blue limestones, and sites 14–16 in the blue–violet limestones. 175 samples from 14 sites were collected in the western limb of the anticline, where the dip is low. Because of the bad outcrop conditions (the major part of the formation is buried by Stephano–Autunian, Triassic and Quaternary deposits), only 27 samples from two sites were sampled on the eastern limb.

One–three specimens were cut from each core in order to have additional specimens for pilot studies and rock magnetic analysis. Prior to any demagnetization analysis, the specimens were put in a zero field for at least one month, in order to reduce existing viscous components. The Natural Remanent Magnetization (NRM) of the specimens was measured using a JR4 spinner magnetometer (Agico, Brno). Several pilot specimens from each site were subjected to a stepwise alternating field (AF) (up to 180×10^{-3} T) or thermal (up to 660 °C) demagnetizations in order to characterize their magnetic behaviour.

The results of the pilot studies were used to discriminate and discard specimens from sites showing only Cenozoic (such as site 6) or Permian (such as site 2) remagnetizations and those from sites (such as site 3) that show unstable remanent magnetization during the demagnetization process. Finally, 132 samples were demagnetized in this study.

The results of the pilot studies showed also that the AF procedure did not allow complete demagnetization. Thermal demagnetization was applied to the remaining specimens. The thermal demagnetization was performed using a cylindrical furnace with a fast heating level while forced air enhanced the cooling. In order to isolate correctly and identify the components of magnetization, numerous steps were performed with increments ranging from 150 °C at the lowest temperatures to 25 °C at the highest temperatures. Demagnetization data analysis was carried out using classical methods: the directions of the magnetization components were plotted on orthogonal vector plots (Wilson & Everitt 1963; Zijderveld 1967); the remaining vectors and vectorial differences of the magnetization were

Downloaded from https://academic.oup.com/gji/article/147/2/343/718535 by guest on 04 March 2022

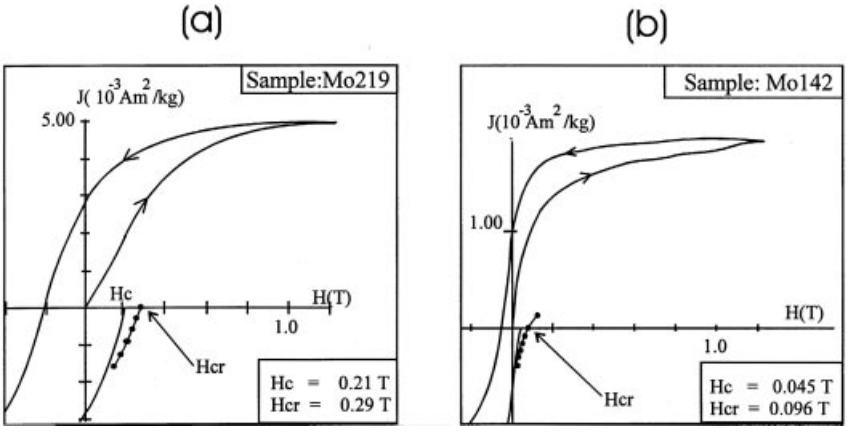


Figure 2. Hysteresis loop: (a) blue–violet limestone; (b) rubefied red clays (H_c: coercive force; H_{cr}: remanent coercive force).

plotted on equal-area projections; the remagnetization circles methods (Halls 1976; Halls 1978; McFadden & McElhinny 1988) were also used. The mean directions of the different components were computed using principal component analysis (Kirschvink 1980), Fisher (1953) statistics and a bivariate form of Fisher statistics (Le Goff 1990; Le Goff *et al.* 1992). For progressive unfolding, the parameters k (Fisher 1953) and $k\delta$ (the value of the precision parameter from the elliptical confidence zone in the direction perpendicular to the fold axis; Henry & Le Goff 1994) were used.

ROCK MAGNETISM

Hysteresis loops were obtained for small cores (cylindrical samples of 1 cm × 1 cm) using a laboratory-made translation inductometer within an electromagnet capable of reaching 1.6 T.

For the blue–violet limestones, saturation of the magnetization is not reached (Fig. 2a) and the coercive force and the remanent coercive force are relatively strong ($H_c = 0.21$ T, $H_{cr} = 0.29$ T). This indicates that the main carrier of the magnetization is haematite or goethite.

The hysteresis loops for the rubefied red clays (Fig. 2b) and the blue–green facies also show that saturation is not reached. The coercive forces are lower ($H_c = 0.045$ T, $H_{cr} = 0.096$ T) for the rubefied clays than for the blue–violet limestones ($H_c = 0.071$ T, $H_{cr} = 0.36$ T). In most cases the loops show a wasp-waisted shape, indicating the existence of at least two different magnetic components, haematite or goethite, and another component with lower coercivity (possible magnetite).

Thermomagnetic curves (low-field susceptibility as a function of temperature) have been determined by heating in air using the CS2 equipment, Kappabridge KLY2 (Agico, Brno). Despite the occurrence of strong mineralogical alteration during the heating in many samples, the Curie curves, in favourable cases, give more precise information about the magnetic carrier. They confirm the presence in the blue–green limestones and in the rubefied red clay facies of haematite and magnetite. Haematite is also shown by blocking temperatures higher than 580 °C. In the example of Fig. 3, the mineralogical alteration revealed by a decrease of susceptibility cannot be due to the formation of magnetite. The observed Curie point at 580 °C, with a small Hopkinson peak, is therefore related to pre-existing magnetite.

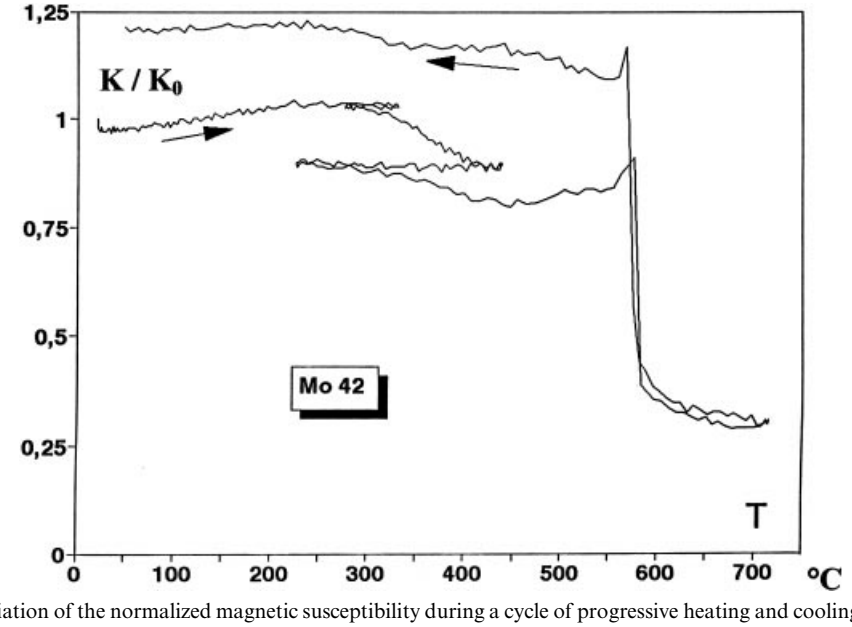


Figure 3. Example of variation of the normalized magnetic susceptibility during a cycle of progressive heating and cooling in air of a sample from the blue and green facies, showing, in addition to a 'Hopkinson' peak related to magnetite, the presence of haematite.

Downloaded from https://academic.oup.com/gji/article/147/2/343/718535 by guest on 04 March 2022

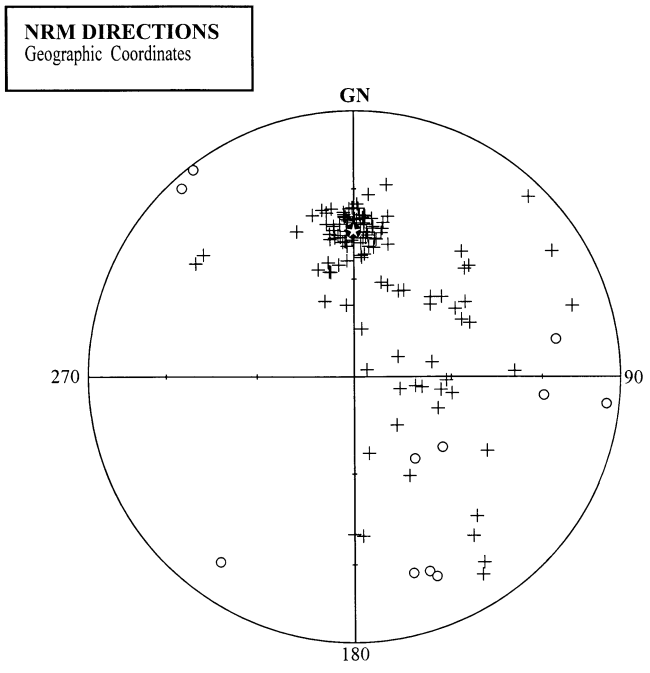


Figure 4. Equal-area plot of the NRM directions for all samples (crosses: positive inclinations; open circles: negative inclinations). Open star: present magnetic field direction.

At temperatures higher than 580 °C, the magnetic susceptibility continues to decrease until temperatures of approximately 670–680 °C, thus confirming the existence of haematite.

The presence of magnetite in the blue–violet limestones is not clearly demonstrated, and the main carrier is haematite. Because of the reversibility of the heating and cooling curves, this haematite is a pre-existing mineral.

Two main magnetic carriers have thus been revealed in the formation studied. Haematite is present in the blue–violet limestones, and both magnetite and haematite are present in the blue–green limestones and in the rubefied red clays.

PALAEOMAGNETIC RESULTS

The NRM directions are distributed on a girdle (Fig. 4). This girdle is elongated between the present Earth magnetic dipole field direction and a SSE direction. This arrangement suggests a superimposition of at least two components in the NRM. NRM intensities values range from 6 to 2373×10^{-4} A m^{-1}, with a mean of 227×10^{-4} A m^{-1} (Fig. 5).

During demagnetization, after eventual elimination of a small viscous component, the analysis of the magnetization directions of the samples gives two different kinds of results: a stable magnetic direction characteristic of an apparently single component, or directions evolving along a great circle, which shows the superimposition of unblocking temperature spectra for at least two components. The analysis of the data indicates that the stable characteristic remanent magnetizations (ChRMs) have different orientations, allowing their separation into three groups (A, of normal polarity only, and B and C, of reversed polarity only).

ChRM analyses

ChRM A

The first ChRM (A), isolated at seven sites, has mean directions defined by $D = 359.8°$, $I = 44.7°$, $k = 178$, $\alpha_{95} = 4.5°$ and $D = 3.4°$, $I = 44.9°$, $k = 54$, $\alpha_{95} = 8.3°$, before and after dip correction, respectively (Table 1). This direction is better grouped in geographical coordinates (for progressive unfolding, the maximum k-value is obtained for -5 per cent unfolding) and is very close to that of the present Earth's magnetic field at the site. The palaeomagnetic pole corresponding to this component before dip correction (88.8°N, 164°E, $K = 262$, $A_{95} = 3.3°$) is close to that from some sites of other formations of the Illizi basin that show Cenozoic remagnetization (82.6°N, 97.6°E, Henry *et al.* 1992; 74.6°N, 73.3°E, Derder *et al.* 1994a). This direction is thus interpreted as a total remagnetization, which occurred during Cenozoic times.

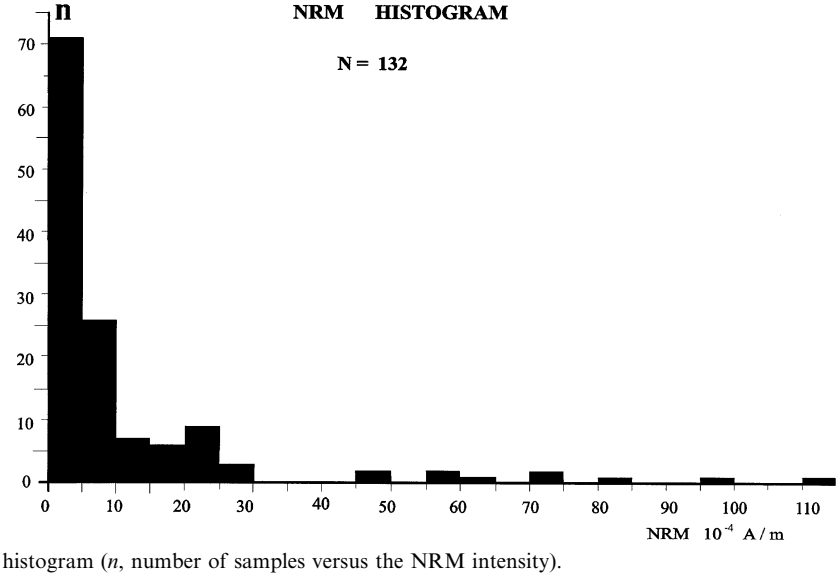


Figure 5. NRM intensity histogram (n, number of samples versus the NRM intensity).

Downloaded from https://academic.oup.com/gji/article/147/2/343/718535 by guest on 04 March 2022

Table 1. ChRMs A and B (Cenozoic and Permian overprints): mean directions (*D, I* in degrees) obtained for each site (*N*: number of samples); palaeomagnetic pole: Lat. (°S), Long (°E); and corresponding Fisher parameters (k, α_{95}, K, A_{95}; α_{95} and A_{95} in degrees).

Before dip correction						After dip correction				Palaeopole			
Site	*N*	*D* (°)	*I* (°)	*k*	α_{95}	*D* (°)	*I* (°)	*k*	α_{95}	Lat (°S)	Long (°E)	*K*	A_{95}
Cenozoic total overprint													
2	2	0.0	50.0	–	–	355.0	55.0	–	–				
5	8	1.9	47.5	77	6.4	1.9	47.4	77	6.4				
6	5	356.4	37.0	612	3.1	356.4	37.0	612	3.1				
8	1	359.0	41.0	–	–	354.0	38.0	–	–				
11	7	0.4	49.7	149	5.0	358.6	52.8	149	5.2				
12	7	1.2	37.7	213	4.1	14.4	34.9	213	4.1				
13	1	0.0	50.0	–	–	22.0	46.0	–	–				
Mean	31	0.2	44.1	82	2.9	3.6	44.5	48	3.8				
Mean	7 sites	359.8	44.7	178	4.5	3.4	44.9	54	8.3				
Mean	7 sites									−88.8	−196.0	262	3.3
Permian overprint													
1	3	149.8	6.5	64	15.5	150.3	2.5	52	17.2				
2	2	144.1	−6.1	–	–	143.4	−8.3	–	–				
9	1	148.7	15.7	–	–	148.7	15.7	–	–				
14	2	148.1	13.5	–	–	148.1	13.5	–	–				
15	6	147.2	11.7	139	5.7	147.2	11.7	139	5.7				
16	1	131.9	16.5	–	–	131.9	16.5	–	–				
Mean	15	146.5	9.2	64	4.8	146.5	9.2	53	5.3				
Mean	6 sites	145.0	9.7	58	8.9	145.0	7.9	38	11.1				
Mean	6 sites									43.4	61.7	93	5.9

ChRM B

The second orientation of the ChRM (B) was isolated at six sites: $D=145.0°$, $I=9.7°$, $k=58$, $k\delta=53$, $\alpha_{95}=8.9°$ and $D=145.0°$, $I=7.9°$, $k=38$, $k\delta=44$, $\alpha_{95}=11.1°$, before and after dip correction, respectively (Table 1). These two directions are not very different and the fold test is of little significance because all the corresponding sites are in the same weakly dipping limb of the fold (taking into account only the precision parameter values, the deformation should be older than the magnetization). The directions are very close to that determined in some sites of the Moscovian El Adeb Larache formation, which show Permian remagnetization directions (Henry *et al.* 1992). In geographical coordinates, this second orientation also yielded a palaeomagnetic pole (43.4°S, 61.7°E, $K=93$, $A_{95}=5.9°$) very close to previous poles of Permian remagnetization determined at El Adeb Larache (42°S, 65.1°E; Henry *et al.* 1992) and in other areas of the Saharan craton, for example at Hassi Bachir (35.5°S, 60°E; Daly & Irving 1983) and at Beni-Abbes (49.5°S, 42.2°E; Aifa 1987). Thus, this component is probably a total magnetic overprint, which was acquired during Permian times.

ChRM C

The third component (C) was isolated from two types of magnetic behaviour. With the first, after the elimination of a small component probably of viscous origin, only a stable orientation of the magnetization (Fig. 6) is observed during the demagnetization process. In the second, the magnetization directions (vectorial differences and/or the remaining vectors) are evolving along great circles (Fig. 7) towards the SE and reach a stable direction C only at the highest temperatures. The ChRM direction defined by this C component, computed from 32 specimens and distributed over six sites, has the following directions: $D=134.8°$, $I=34.2°$, $k=96$, $k\delta=66$, $\alpha_{95}=6.9°$ and $D=133.7°$, $I=32.6°$, $k=254$, $k\delta=332$, $\alpha_{95}=4.2°$, before and after dip correction, respectively (Table 2). The maximum value of the precision parameter during progressive unfolding is obtained for 92 per cent unfolding ($k\delta=341$). The difference between $k\delta$ values for 92 and 100 per cent unfolding is statistically not significant, and the simple and stringent McElhinny (1964) fold test is positive and significant at the 99 per cent level.

Direction of the C component from great-circles analyses

For most of the samples that show an evolution along great circles of their magnetization directions during demagnetization (superimposition of unblocking temperature spectra for at least two components), a stable direction was not reached, even at high temperatures (Fig. 8), and only the great-circles data are available. The analysis of remagnetization circles using Halls' method (Halls 1976, 1978) was thus applied. The intersection direction obtained appears to be relatively similar in the three sites (Table 3). There is a coincidence between these intersections and the ChRM directions determined in other samples of the same sites (Table 2). A similarity also exists between the direction obtained from all the ChRM data (Fig. 9 and Table 2) and that obtained by the best intersection using all the available circles (Figs 10a and c). This result shows that the McFadden & McElhinny (1988) approach is therefore useable here to integrate great circles and ChRM data within each site (Table 4).

The confidence zone of the best intersection direction (Henry 1999) for all the great circles is much smaller after dip correction than before (Figs 10b and d). This is another argument in favour of a positive fold test (Fig. 11).

Downloaded from https://academic.oup.com/gji/article/147/2/343/718535 by guest on 04 March 2022

Table 2. ChRM C (Moscovian directions); see Table 1.

Before dip correction						After dip correction				Palaeopole			
Site	*N*	*D* (°)	*I* (°)	*k*	α_{95}	*D* (°)	*I* (°)	*k*	α_{95}	Lat (°S)	Long (°E)	*K*	A_{95}
1	3	134.4	33.8	468	5.7	138.3	32.4	468	5.7				
5	8	136.9	35.8	39	10.0	136.0	35.8	39	10.0				
8	2	127.5	30.2	–	–	127.5	36.0	–	–				
13	5	143.0	47.1	148	6.3	130.3	33.4	148	6.3				
14	10	136.9	31.5	64	6.1	136.9	31.5	64	6.1				
16	4	132.4	26.2	91	9.7	132.4	26.2	91	9.7				
Mean	32	136.2	34.5	48	3.7	134.9	32.6	62	3.3				
Mean	6 sites	134.8	34.2	96	6.9	133.7	32.6	254	4.2				
Mean	6 sites									25.6	59.5	381	2.9

Direction of the C component from the ChRM and the great circles

There is a remarkable coincidence in the results obtained with different approaches. For example, after dip correction, the mean direction is

$D = 134.9°$, $I = 32.6°$, $k = 62$, $\alpha_{95} = 3.3°$ (32 samples) for ChRM C (Table 2);

$D = 134.5°$, $I = 35.8°$ (21 circles from five sites) for the great circles only (Table 3);

$D = 135.7°$, $I = 32.6°$, $k = 70$, $\alpha_{95} = 2.4°$ for a combination of the ChRM and the great circles (McFadden & McElhinny 1988).

Finally, the mean direction for all seven sites has been calculated (using the mean ChRM for sites 14 and 16, the mean ChRM combined with great circles for sites 1, 5, 8 and 13, and the mean from the great circles only for site 12): $D = 138.0°$, $I = 33.7°$, $k = 59$, $k\delta = 58$, $\alpha_{95} = 6.9°$ and $D = 136.1°$, $I = 31.2°$, $k = 130$, $k\delta = 424$, $\alpha_{95} = 4.6°$, before and after dip correction, respectively (Fig. 12). The fold test for these data (Fig. 13) is again positive and significant (at the 99 per cent level for $k\delta$;

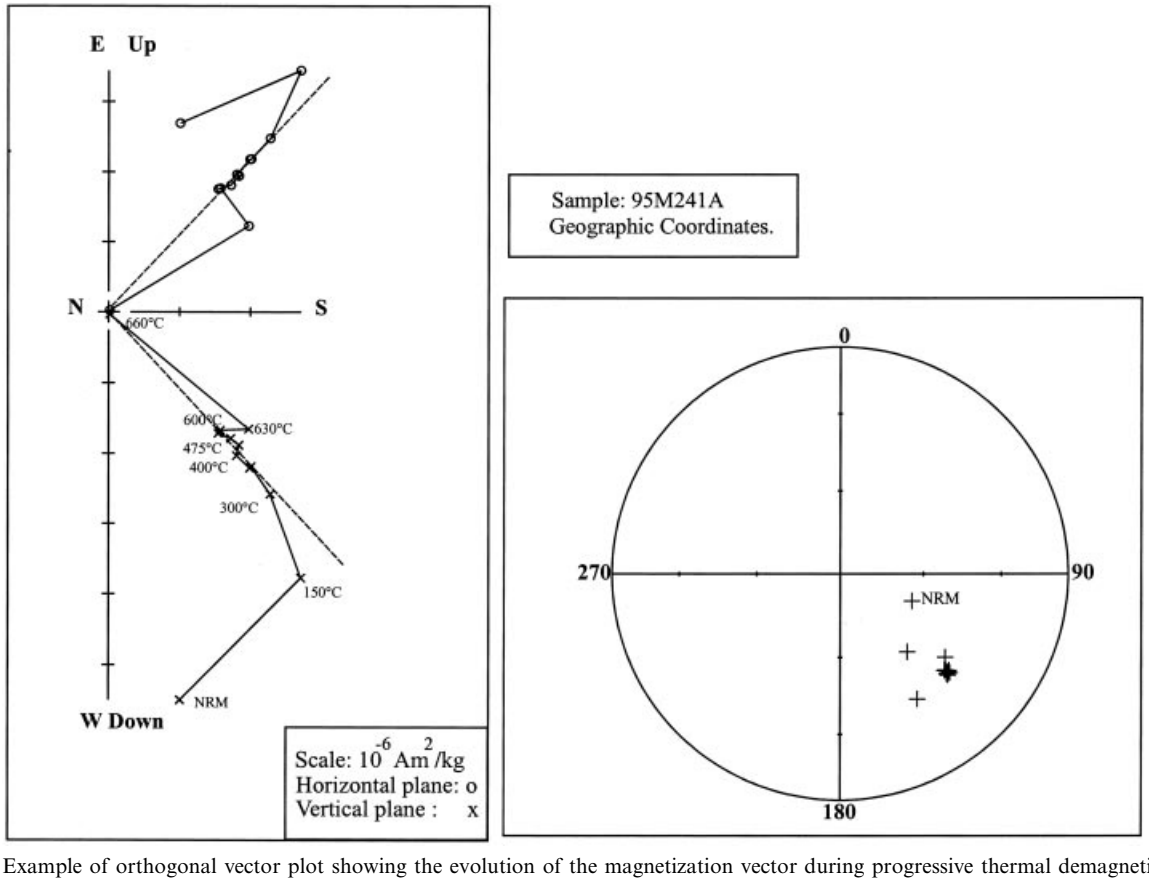


Figure 6. Example of orthogonal vector plot showing the evolution of the magnetization vector during progressive thermal demagnetization for sample 95M241A [projection on horizontal (open symbols) and vertical (crosses) planes] and an equal-area plot (crosses: positive inclinations) showing a stable magnetic direction.

Downloaded from https://academic.oup.com/gji/article/147/2/343/718535 by guest on 04 March 2022

Table 3. Mean direction (*D, I* in degrees) obtained from each site (*N*: number of samples) using the remagnetization circles analysis of Halls (1976, 1978).

Before dip correction						After dip correction			
Site	*N*	*D* (°)	*I* (°)	*k*	α_{95}	*D* (°)	*I* (°)	*k*	α_{95}
5	4	125.3	46.3			125.3	46.3		
12	5	155.8	31.2			147.6	22.6		
13	3	158.8	30.5			149.6	22.0		
Mean	21*	1.3	44.7			134.5	35.8		
Mean	3 sites	148.3	36.9	23	16.8	142.3	30.7	21	10.1

* For the calculation of the best intersection using all the great circles, two circles from site 4 and two circles from site 11 have been integrated.

McElhinny 1964) and the maximum values of $k\delta$ and k are obtained for unfolding of 111 per cent ($k\delta = 452$) and 98 per cent ($k = 131$), respectively. These values are not statistically different from those obtained at 100 per cent unfolding. The associated palaeomagnetic pole is situated at 28.3°S, 58.9°E, $K = 157$, $A_{95} = 4.2°$.

DISCUSSION

This positive fold test confirms the early character of magnetization C, which was acquired before the first tectonic episode. This episode is older than the Upper Triassic, and started before or during the Stephano–Autunian (Attar *et al.* 1981). The rather negative fold test obtained for the Permian

Table 4. Mean direction (*D*, *I* in degrees) obtained from each site using a combination of remagnetization circles and ChRM (McFadden & McElhinny 1988) (*N*: number of great circles; *n*: number of ChRMs). Palaeomagnetic pole: Lat. (°S), Long (°E) and corresponding Fisher parameters (*k*, α95, *K* and A_{95}; α_{95} and A_{95} in degrees).

Before dip correction							After dip correction				Palaeopole			
Site	*N*	*n*	*D* (°)	*I* (°)	*k*	α_{95}	*D* (°)	*I* (°)	*k*	α_{95}	Lat (°S)	Long (°E)	*K*	A_{95}
1	2	3	132.2	32.6	210	5.7	135.9	31.6	211	5.7				
5	4	8	136.8	35.5	38	7.2	136.8	35.5	38	7.2				
8	3	2	127.6	29.3	172	6.7	128.5	35.1	172	6.7				
12	5	–	155.8	31.2	–	–	147.6	22.6	–	–				
13	3	5	147.2	47.8	139	4.9	133.4	34.8	140	4.8				
Mean	17 sp.	32	138.4	35.0	40	3.3	135.7	32.6	70	2.4				
Mean	6 sites		139.6	35.7	46	9.3	136.7	32.1	99	6.3				
Mean	6 sites										28.2	58.0	116	5.8

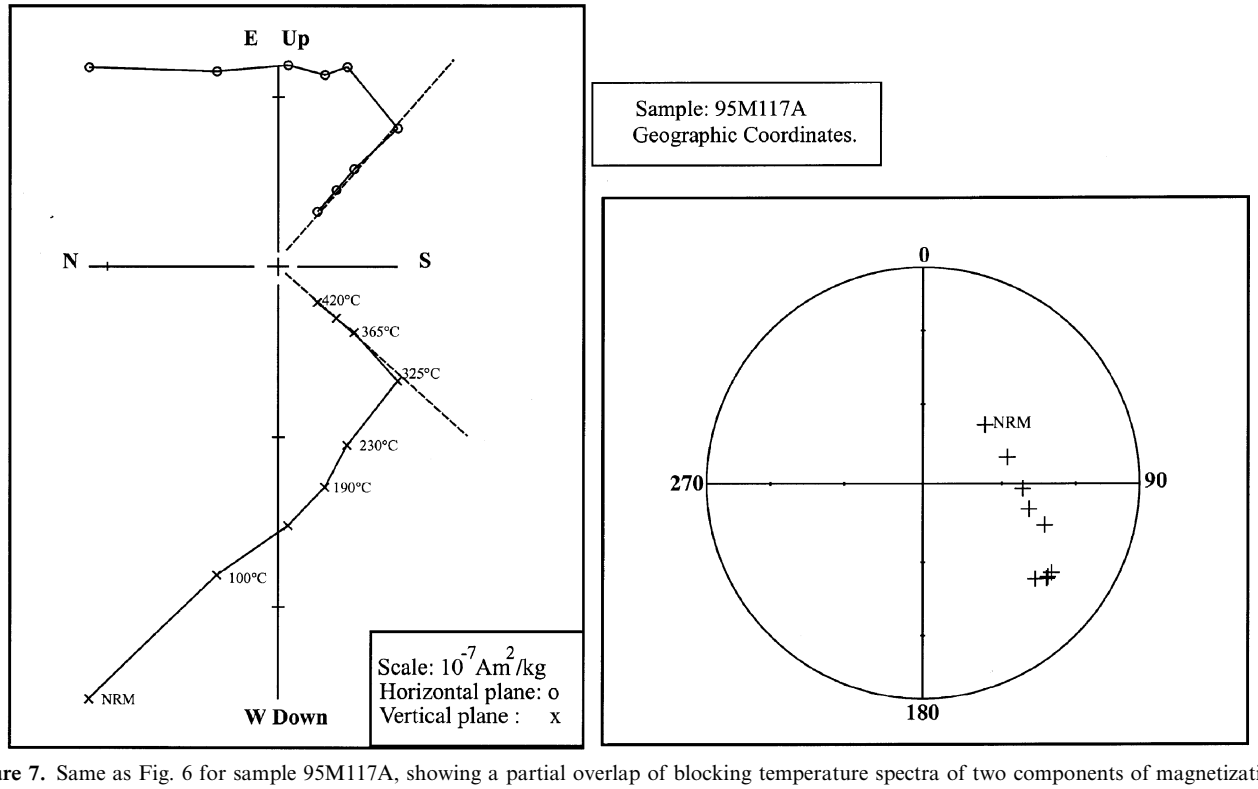


Figure 7. Same as Fig. 6 for sample 95M117A, showing a partial overlap of blocking temperature spectra of two components of magnetization.

Downloaded from https://academic.oup.com/gji/article/147/2/343/718535 by guest on 04 March 2022

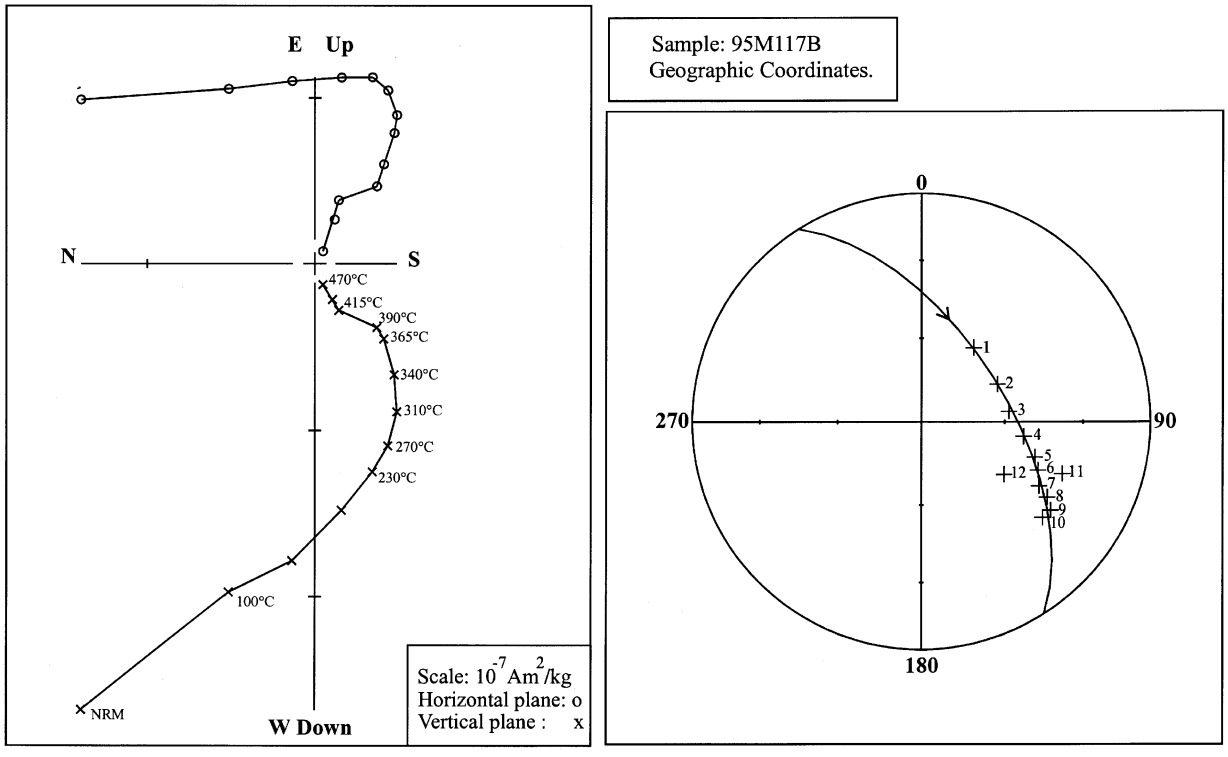


Figure 8. Same as Fig. 6 for sample 95M117B, showing a total overlap of blocking temperature spectra of two components of magnetization.

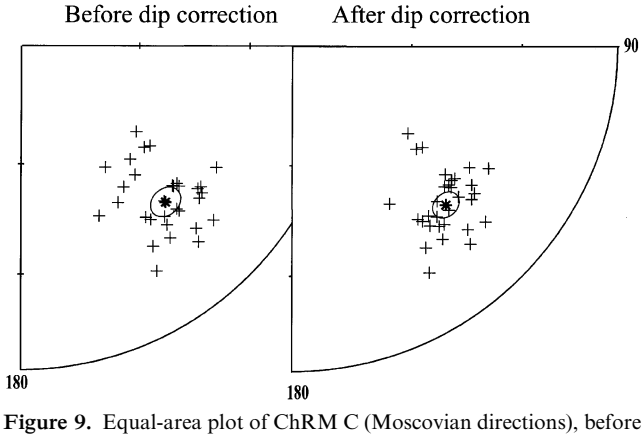


Figure 9. Equal-area plot of ChRM C (Moscovian directions), before and after dip correction (crosses: positive inclinations).

component also argues for an Upper Carboniferous or Early Permian age for the folding. The isolation of this Permian overprint (B) in part of the samples shows that component C cannot be the result of this widespread Permian remagnetization. Component C thus represents the primary magnetization of these Moscovian rocks. Since it was obtained from several levels of the Moscovian, it therefore constitutes a new and significant contribution for Moscovian times.

Ignoring the 'Dwyka pole' (McElhinny & Opdyke 1968) of doubtful age (see Henry *et al.* 1992), the palaeomagnetic pole associated with the primary component of this study (28.3°S, 58.9°E) is in good agreement with the corresponding segment of the African apparent polar wander path (Besse *et al.* 1996; Chen *et al.* 1994; Smith *et al.* 1994). Indeed, it is very close to the palaeomagnetic poles for stable Africa (Table 5) from the same period and for neighbouring periods (Fig. 14): the

Table 5. Middle and Upper Carboniferous palaeomagnetic poles for stable Africa.

Symbol	Age	Rock unit	Lat (°S)	Long (°E)	A_{95}	Reference
HB	Upper Namurian–Lower Moscovian	Hassi Bachir	26.8	56.6	3.7	Daly & Irving (1983)
AIN1	Lower Moscovian	Aïn Ech Chebbi	22.9	51.8	6.3	Daly & Irving (1983)
EAL	Moscovian	El Adeb Larache	28.7	55.9	2.9	Henry *et al.* (1992)
RN	Namurian	Reouina	28.4	56.9	1.7	Merabet *et al.* (1999)
MK	Lower Stephanian	Merkala	32.4	56.6	2.3	Henry *et al.* (1999)
OB	Bashkirian	Oubarakat	28.2	55.5	3.4	Derder *et al.* (2001a)
AIN2	Middle Carboniferous	Aïn Ech Chebbi	26.5	44.7	4.7	Derder *et al.* (2001b)
EDJ	Moscovian	Edjeleh	28.3	58.9	4.2	this study

Downloaded from https://academic.oup.com/gji/article/147/2/343/718535 by guest on 04 March 2022

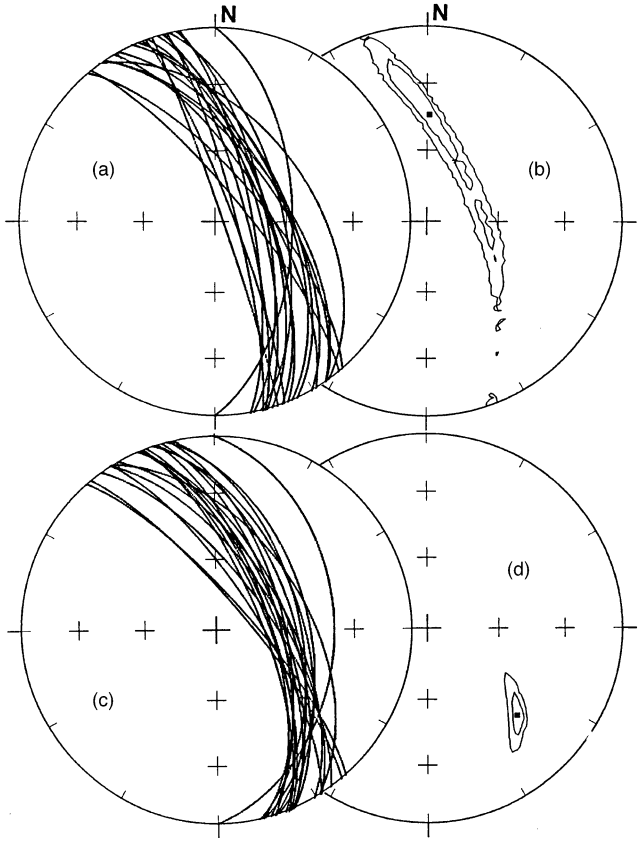


Figure 10. Remagnetization circles (a, c) and their corresponding confidence zones at 63 per cent and 95 per cent (Henry 1999) for their best intersection (b, d) obtained from 21 specimens distributed over five sites (equal-area plot, lower hemisphere), in geographical (a, b) and stratigraphic (c, d) coordinates.

Upper Namurian–Lower Moscovian pole (26.8°S, 56.6°E; Daly & Irving 1983) at Hassi Bachir (Ahnet basin), the Lower Moscovian pole (22.9°S, 51.8°E; Daly & Irving 1983) of Aïn Ech Chebbi (Reggane basin), the Moscovian pole (28.7°S, 55.9°E; Henry *et al.* 1992) at El Adeb Larache (Illizi basin), the Namurian pole (28.4°S, 56.9°E; Merabet *et al.* 1999) at Reouiana (Tindouf basin), the Lower Stephanian pole (32.4°S, 56.6°E; Henry *et al.* 1999) at Merkala (Tindouf basin) and the Bashkirian pole (28.4°S, 57.1°E; Derder *et al.* 2001a) at Oubarakat (Illizi

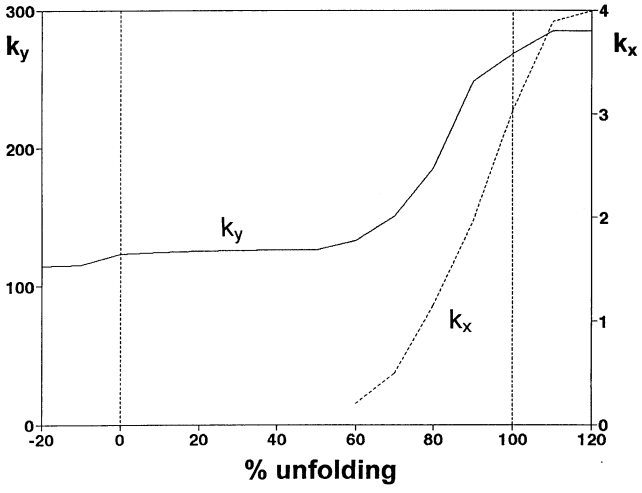


Figure 11. Variation of k_y and k_x (Le Goff 1990; Le Goff *et al.* 1992) parameters from great circles (Henry 1999) during progressive unfolding. The k_x values are of little significance because of the scattering of the best intersections within the plane corresponding to most of the great circles.

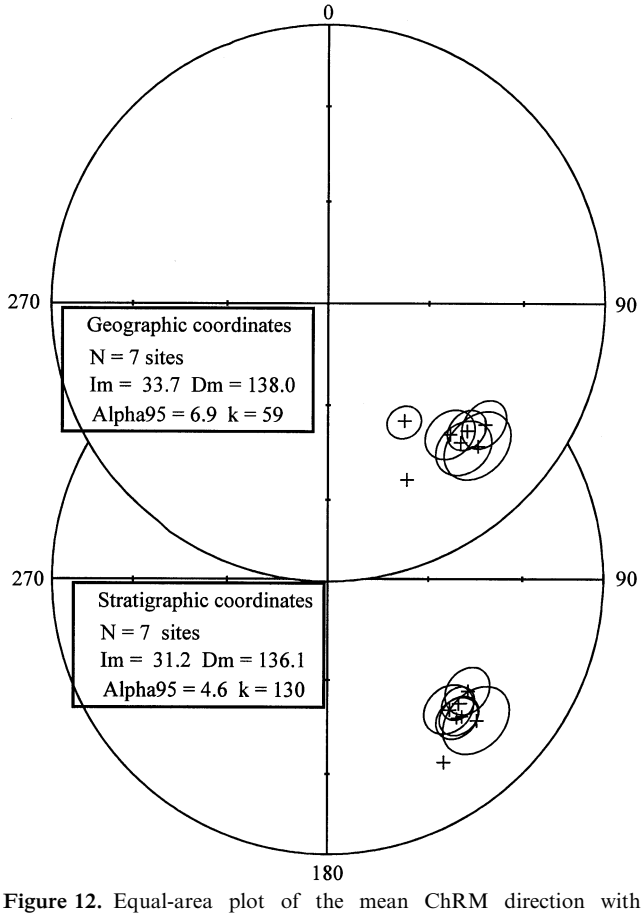


Figure 12. Equal-area plot of the mean ChRM direction with associated 95 per cent confidence zone at each site, in geographical and stratigraphic coordinates (Tables 3 and 4). The direction without confidence zone is that obtained from site 12 using Halls' (1976) method (Table 3).

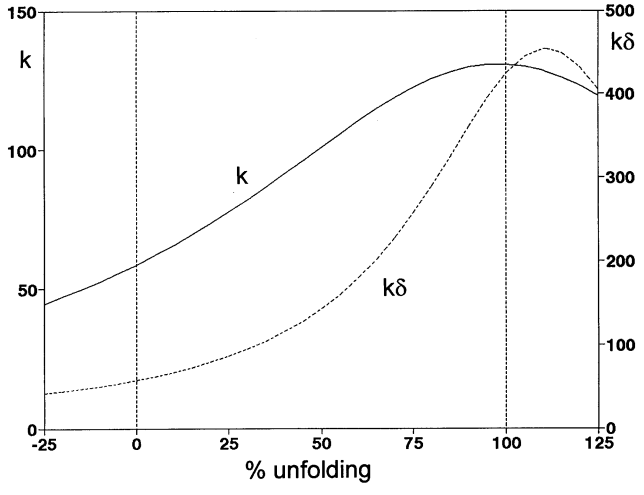


Figure 13. Variation of $k\delta$ (Henry & Le Goff 1994) and k (Fisher 1953) parameters during progressive unfolding.

Downloaded from https://academic.oup.com/gji/article/147/2/343/718535 by guest on 04 March 2022

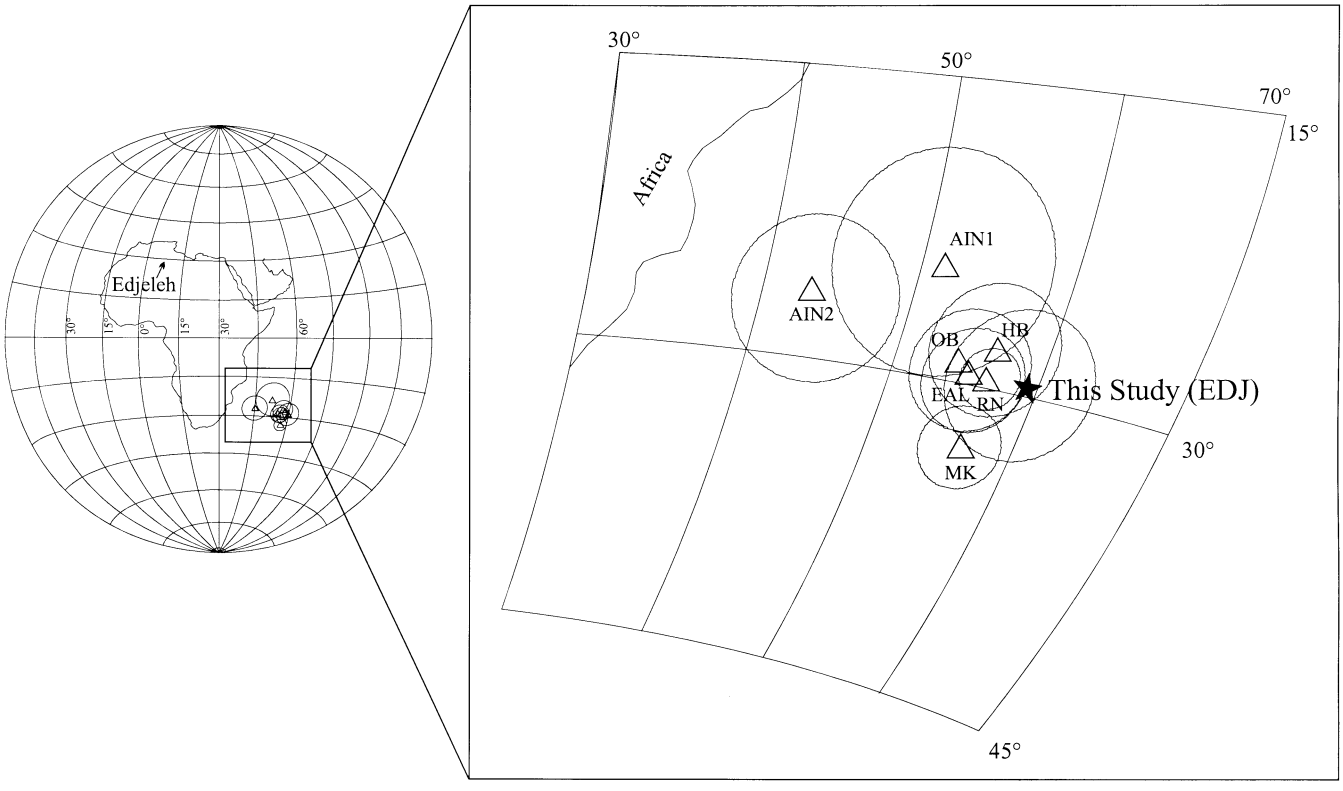


Figure 14. African Middle to Upper Carboniferous palaeomagnetic poles (see Table 5).

basin). However, unlike all these poles, the age of the Edjeleh pole is constrained by a palaeomagnetic test. These new results thus confirm the reliability of the previous poles and validate them.

This datum is not far from a new pole (with both positive reversal and fold tests) of Middle Carboniferous age (26.5°S, 44.7°E, $K=383$, $A_{95}=4.7°$; Fig. 14) determined recently (Derder *et al.* 2001b) in the Bled El Mass region (near the Ain Ech Chebbi area, Reggane basin).

It should be noted that all the African Upper Carboniferous poles are in fact obtained from the Saharan platform. The coherence observed between these data obtained from distant places of this wide platform (Illizi basin is situated in the eastern part of this platform, Ahnet and Reggane basins in the central part and Tindouf basin in the western part; Fig. 1b) leads to a very good knowledge of the Namuro–Westphalian part of the apparent polar wander path for Africa, and in particular for the North African craton (Ricou & Besse 1998).

CONCLUSIONS

As in most of the previous palaeomagnetic studies of the Saharan platform, the results obtained in the well-dated marine Moscovian formation at Edjeleh show the existence of Cenozoic and Permian remagnetization events. The primary remanent magnetization was also isolated and its acquisition age confirmed by a positive fold test. The corresponding palaeomagnetic pole (28.3°S, 58.9°E, $K=157$, $A_{95}=4.2°$) thus constitutes, with the recent datum of Bled El Mass, the first African Upper Carboniferous pole with an age constrained by a statistical positive fold test. Because it is in good agreement with the previously published African poles for neighbouring periods determined without palaeomagnetic tests, it confirms their reliability.

When combined with previous Gondwana poles, the new datum deduced from this study reinforces the recent result of Derder *et al.* (2001a), which shows that a better reconstruction is obtained for Gondwana for this interval of time if Ricou's parameters (Ricou *et al.* 1990) are used rather than those from the classical model of Du Toit (1937).

This new result also confirms the model of Matte (1986) and Henry *et al.* (1992), which stipulates that the latitudinal displacement of Africa during the Carboniferous was mainly related to a large clockwise rotation (about 25°). This model, which explains the evolution of the main collision area between Gondwana and Laurussia during the Carboniferous, is more compatible with the Permian Pangaea A2 reconstruction (Van der Voo 1981).

The results obtained in this study and in that undertaken in the Bled El Mass region (Reggane basin; Derder *et al.* 2001b) underline the value of investigating folded areas in cratonic regions. This is why the folded Hassi Bachir Formation of Upper Namurian–Lower Moscovian age (Ahnet basin) must be revisited in order to determine a more reliable Upper Carboniferous African pole by studying this geological formation in more detail than in the Daly & Irving (1983) study.

ACKNOWLEDGMENTS

We are very grateful to the Sonatrach Production Department, especially Mr Sahar and Mr Benslama (head of In Amenas base) and to Mr Touba for his help with the fieldwork. Our

Downloaded from https://academic.oup.com/gji/article/147/2/343/718535 by guest on 04 March 2022

thanks also go to Mansour Bina and Henri Rouvier for their help in measurement of the samples and to Haydar Aziz Baker for help with the manuscript. Thanks also to Heinrich Soffel and an anonymous referee for their constructive reviews.

REFERENCES

Achab, A., 1970. Le Permo-Trias saharien, Associations palynologiques et leurs applications en stratigraphie, *Thesis,* Algiers University, Algiers.

Aifa, T., 1987. Paléomagnétisme en zones de collision: déformations récentes dans l'arc Tyrrhénien et raccourcissement crustal hercynien en Afrique, *Thesis,* Paris 7 University, Paris.

Attar, A., Fabre, J., Janvier, P. & Lehmann, J.P., 1981. Les vertébrés de la formation de Tiguentourine (Permo-Carbonifère, bassin d'Illizi, Algerie), *Bull. Muséum Natl d'Histoire Naturelle Paris,* 4eme Serie, **3C,** 301–309.

Besse, J., Théveniaut, H. & Courtillot, V., 1996. Apparent polar wandering paths for North America, Africa, Laurussia and West Gondwana since the Upper Carboniferous: a review, in *Tethys Paleoenvironments, Ocean Basins and Margins,* pp. 71–97, ed. Nairn, A.E.M., Plenum Press, New York.

Chen, Z., Li, Z.H., Powell, C.M. & Balme, B.E., 1994. An Early Carboniferous paleomagnetic pole for Gondwanaland: new results from the Mount Eclipse Sandstone in the Ngalia Basin, central Australia, *J. geophys. Res.,* **99** (B2), 2909–2924.

CRZA & CNRS, 1965. *Geological Map of Illizi (Fort de Polignac),* Carte géologique de l'Algérie, Map NG 32 NO-NE, 1: 500 000.

Daly, L. & Irving, E., 1983. Paléomagnétisme des roches carbonifères du Sahara central; analyse des aimantations juxtaposées; configurations de la Pangée, *Ann. Geophys.,* **1,** 207–216.

de Lapparent, A.F., 1949. Première description géologique de l'Edjeleh Tan In Azzaoua (N.E de l'Ajjers, Sahara), *Ann. Soc. Géol. Du Nord,* **69,** 86–89.

Derder, M.E.M., Henry, B., Merabet, N. & Daly, L., 1994a. Paleomagnetism of the Stephano–Autunian Lower Tiguentourine Formations from stable Saharan craton (Algeria), *Geophys. J. Int.,* **116,** 12–22.

Derder, M.E.M., Henry, B. & Merabet, N., 1994b. Paleomagnetism of the Middle Zarzaïtine formation of Liassic-Dogger age from the stable Saharan craton (Illizi Basin, Algeria), in *XIXth Gen. Assemb. EGS,* p. 121, Grenoble, France.

Derder, M.E.M., Henry, B., Merabet, N., Amenna, M. & Bourouis, S., 2001a. Upper Carboniferous palaeomagnetic pole from stable Saharan craton and the Gondwana reconstructions, *J. African Earth Sci.,* in press.

Derder, M.E.M., Smith, B., Henry, B., Yelles, A.K., Bayou, B., Djellit, H., Ait Ouali, R. & Gandriche, H., 2001b. Juxtaposed and superimposed paleomagnetic primary and secondary components from the folded Middle Carboniferous sediments in the Reggane Basin (Saharan craton, Algeria), *Tectonophysics,* **332,** 403–422.

Durif, P., 1959. Observations micropaléontologiques (foraminifères) sur le Carbonifère marin du bassin de Fort de Polignac (Sahara oriental), *Bull. Soc. Geol. Fr.,* **7,** 163–165.

Du Toit, A.L., 1937. *Our Wandering Continents, an Hypothesis of Continental Drifting,* Oliver and Boyd, Edinburgh.

Fisher, R.A., 1953. Dispersion on a sphere, *Proc. R. Soc. Lond.,* **A217,** 295–305.

Halls, H.C., 1976. A least squares method to find a remanence direction from converging remagnetization circles, *Geophys. J. R. astr. Soc.,* **45,** 297–304.

Halls, H.C., 1978. The use of converging remagnetization circles in paleomagnetism, *Phys. Earth planet. Inter.,* **16,** 1–11.

Henry, B., 1999. Confidence zone from remagnetization circles: a new possibility for the fold tests, *Euro. Un. Geosci.,* Vol. 10, Strasbourg, France.

Henry, B. & Le Goff, M., 1994. A new tool for palaeomagnetic interpretation: the bivariate extension of the Fisher statistics, *XIXth Gen. Assemb. EGS,* p. 123, Grenoble, France.

Henry, B., Merabet, N., Yelles, A., Derder, M.E.M. & Daly, L., 1992. Geodynamical implications of a Moscovian palaeomagnetic pole from the stable Sahara craton (Illizi basin, Algeria), *Tectonophysics,* **201,** 83–96.

Henry, B., Merabet, N., Bouabdallah, H. & Maouche, S., 1999. Nouveau pôle paléomagnétique stéphanien inférieur pour le craton saharien (Formation de Merkala, bassin de Tindouf, Algérie), *C. R. Acad. Sci. Paris,* **329, IIa,** 161–166.

Kies, B., Henry, B., Merabet, N., Derder, M.M. & Daly, L., 1995. A new Late Triassic–Liassic palaeomagnetic pole from superimposed and juxtaposed magnetizations in the Saharan craton, *Geophys. J. Int.,* **120,** 433–444.

Kirschvink, J.L., 1980. The least-squares line and plane analysis of palaeomagnetic data, *Geophys. J. R. astr. Soc.,* **62,** 699–718.

Le Goff, M., 1990. Lissage et limites d'incertitude des courbes de migration polaire; pondération des données et extension bivariate de la statistique de Fisher, *C. R. Acad. Sci. Paris,* **311** (II), 1191–1198.

Le Goff, M., Henry, B. & Daly, L., 1992. Practical method for drawing a VGP path, *Phys. Earth planet. Inter.,* **70,** 201–204.

Legrand-Blain, M., 1980. Le Carbonifère marin du bassin d'Illizi (Sahara algérien oriental), Mise au point stratigraphique, *C. R. Somm. Soc. Géol. Fr.,* **3,** 81–83.

Matte, P., 1986. La chaîne varisque parmi les chaînes paléozoïques péri-atlantiques, modèle d'évolution et position des grands blocs continentaux au Permo-Carbonifère, *Bull. Soc. Géol. Fr.,* **8,** 9–24.

McElhinny, M.W., 1964. Statistical significance of the fold test in paleomagnetism, *Geophys. J. R. astr. Soc.,* **8,** 338–340.

McElhinny, M.W. & Opdyke, N.D., 1968. The paleomagnetism of some Carboniferous glacial varves from Central Africa, *J. geophys. Res.,* **73,** 689–696.

McFadden, P.L. & McElhinny, M.W., 1988. The combined analysis of remagnetization circles and direct observations in palaeomagnetism, *Earth planet Sci. Lett.,* **87,** 161–172.

Merabet, N., Henry, B., Bouabdallah, H. & Maouche, S., 1999. Paleomagnetism of the Djebel Reouiana Namurian formation (Tindouf Basin, Algeria), *Stud. Geophys. Geodaet.,* **43,** 376–389.

Odin, G.S., 1994. Geological time scale, *C. R. Acad. Sci. Paris,* **318,** 59–71.

Ricou, L.E. & Besse, J., 1998. Improving the fit of Gondwana, *J. African Earth Sci.,* **27,** 159.

Ricou, L.E., Besse, J., Marcoux, J. & Patriat, P., 1990. Une reconstruction du Gondwana révisée à partir de données pluri-disciplinaires, *C. R. Acad. Sci. Paris,* **311,** 463–469.

Smith, B., Moussine-Pouchkine, A. & Ait Kaci Ahmed, A., 1994. Paleomagnetic investigation of Middle Devonian limestones of Algeria and the Gondwana reconstruction, *Geophys. J. Int.,* **119,** 166–186.

Van der Voo, R., 1981. A paleomagnetic comparison of various reconstructions of the Atlantic bordering continents which have implications for the origin of the Gulf of Mexico, *Houston geol. Soc. Continuing Edu. Ser., Proc. Symp.,* pp. 19–20.

Wilson, R.L. & Everitt, C.W.F., 1963. Thermal demagnetization of some carboniferous lavas for palaeomagnetic purposes, *Geophys. J. R. astr. Soc.,* **8,** 149–164.

Zijderveld, J.D.A., 1967. AC demagnetization of rocks: analysis of results, in *Method in Paleomagnetism,* pp. 254–286, eds Collinson, D.W., Creer, K.M. & Runcorn, S.K., Elsevier, Amsterdam.

Downloaded from https://academic.oup.com/gji/article/147/2/343/718535 by guest on 04 March 2022